Neuroimaging in tremor and functional motor disorders

Broersma, Marja

Chapter 4

Motor network disruption in essential tremor: a functional and effective connectivity study

M. Broersma,*[1,2] A.M.M. van der Stouwe,*[1,2] A.W.G. Buijink,*[3,4] S. Sharifi,[3,4] P.F.C. Groot,[4,5] J.D. Speelman,[3] N.M. Maurits,[1,2] A.F. van Rootselaar[3,4]

[1] Department of Neurology, University Medical Center Groningen, University of Groningen, the Netherlands.

[2] Neuroimaging Center, University Medical Center Groningen, University of Groningen, the Netherlands.

[3] Department of Neurology and Clinical Neurophysiology, Academic Medical Center, University of Amsterdam, the Netherlands.

[4] Brain Imaging Center, Academic Medical Center, University of Amsterdam, the Netherlands.

[5] Department of Radiology, Academic Medical Center, University of Amsterdam, the Netherlands.

*Shared first authors

Brain.2015 Oct;138(10):2934-2947

ABSTRACT

BACKGROUND Although involvement of the cerebello-thalamo-cortical network has often been suggested in essential tremor, the source of oscillatory activity remains largely unknown. To elucidate mechanisms of tremor generation, it is of crucial importance to study the dynamics within the cerebello-thalamo-cortical network. Using a combination of electromyography and functional magnetic resonance imaging, it is possible to record the peripheral manifestation of tremor simultaneously with brain activity related to tremor generation.

OBJECTIVE Our first aim was to study the intrinsic activity of regions within the cerebello-thalamo-cortical network using dynamic causal modelling to estimate effective connectivity driven by the concurrently recorded tremor signal. Our second aim was to objectify how the functional integrity of the cerebello-thalamo-cortical network is affected in essential tremor.

METHODS We investigated the functional connectivity between cerebellar and cortical motor regions showing activations during a motor task. Twenty-two essential tremor patients and 22 healthy controls were analysed. For the effective connectivity analysis, a network of tremor-signal related regions was constructed, consisting of the left primary motor cortex, premotor cortex, supplementary motor area, left thalamus, and right cerebellar motor regions lobule V and lobule VIII. A measure of variation in tremor severity over time, derived from the electromyogram, was included as modulatory input on intrinsic connections and on the extrinsic cerebello-thalamic connections, giving a total of 128 models. Bayesian model selection and random effects Bayesian model averaging were used. Separate seed-based functional connectivity analyses for the left primary motor cortex, left supplementary motor area and right cerebellar lobules IV, V, VI and VIII were performed.

RESULTS We report two novel findings that support an important role for the cerebellar system in the pathophysiology of essential tremor. First, in the effective connectivity analysis, tremor variation during the motor task has an excitatory effect on both the extrinsic connection from cerebellar lobule V to the thalamus, and the intrinsic activity of cerebellar lobule V and thalamus. Second, the functional integrity of the motor network is affected in essential tremor, with a decrease in functional connectivity between cortical and cerebellar motor regions. This decrease in functional connectivity, related to the motor task, correlates with an increase in clinical tremor severity. Interestingly, increased functional connectivity between right cerebellar lobules I–IV and the left thalamus correlates with an increase in clinical tremor severity.

CONCLUSIONS In conclusion, our findings suggest that cerebello-dentato-thalamic activity and cerebello-cortical connectivity is disturbed in essential tremor, supporting previous evidence of functional cerebellar changes in essential tremor.

4.1 INTRODUCTION

Essential tremor is one of the most common neurological disorders, and is characterized by a progressive postural and kinetic tremor.[1] Evidence of alleviation of tremor following thalamic deep brain stimulation, and after stroke anywhere in the cerebello-thalamo-cortical network, prompted the hypothesis of essential tremor as an 'oscillating network' disorder.[2,3] Evidence is accumulating that the cerebellum plays an important role in the pathophysiology of essential tremor.[4-6] An important supportive feature is the positive effect of alcohol on essential tremor.[7] Furthermore, emerging clinical features such as ataxic gait,[8-10] eye movement abnormalities[11–13] and intention tremor[14,15] all point to cerebellar changes in essential tremor. Whether these abnormalities relate to structural or functional cerebellar changes is under debate. Pathology studies show an incongruent picture, but provide evidence for neurodegeneration of the cerebellum.[16] There is evidence for morphometric changes and possibly loss of Purkinje cells.[17-20] Moreover, changes in the dentate nucleus have been established, with decreased numbers of GABA receptors reported in essential tremor cases.[21] On the other hand, imaging studies show a striking lack of convincing structural involvement, but do provide evidence for functional abnormalities of the cerebellum (see Sharifi et al, 2014[22] for a review). Although the notional involvement of the cerebellothalamo-cortical network, and of the cerebellum in particular, is becoming increasingly evident, the source of oscillatory activity in essential tremor remains largely unknown.[23,24] To elucidate the mechanisms of tremor generation it is of crucial importance to study network dynamics within the cerebello-thalamo-cortical network. Using a combination of EMG and functional MRI (EMG-fMRI), we can record the peripheral manifestation of tremor simultaneously with brain activity related to tremor generation. Previous studies by our group and others have proven that EMG-fMRI allows identification of brain areas involved in the generation of tremor.[25-28] In a recent EMG-fMRI study, we have demonstrated tremor related increases in activations in specific somatomotor regions of the bilateral cerebellum in essential tremor.[29] In the current, complementary study, we investigate effective and functional connectivity within the tremor network, incorporating information from the concurrently recorded EMG signals to provide better insight into changes within the cerebello-thalamo-cortical network in essential tremor. While functional connectivity describes simple correlations between spatially segregated neuronal events, effective connectivity tries to estimate the underlying, direct, causal connections, which is of crucial importance in the investigation of the underlying biological network.[30] Our first aim was to study intrinsic activity of regions within the cerebello-thalamo-cortical network by using an effective connectivity analysis called dynamic causal modelling (DCM). DCM explores how observed brain activations are generated by estimating the effective connectivity between and within specified regions of interest.[31] For instance, DCM has been shown to be able to identify the correct neural driver behind epileptic seizures by including the occurrence of spike-and-wave discharges obtained from concurrently recorded EEG signals into the model.[32] We hypothesize that internal

cerebellar feedback is altered in essential tremor. The cerebellum is thought to have multiple somatotopic representations.[33] However, until now these have not been studied nor discussed separately in essential tremor. Hence, we will look specifically at intrinsic feedback changes within the anterior motor regions, composed of cerebellar lobules I to V, and posterior motor regions, mainly composed of cerebellar lobule VIII, of the cerebellum.[33] Our second aim was to objectify how the functional integrity of the cerebello-thalamo-cortical network is affected by any cerebellar changes in essential tremor, by means of a functional connectivity analysis, investigating the functional connections between cerebellar and cortical motor regions using a seed-based correlation approach.[27,33] As suggested in a previous study, due to altered cerebellar functioning, we expected to find consequential alterations to functional connectivity between cerebellar and cortical motor regions in essential tremor.[34]

Advancing insights strongly suggest that patients with essential tremor form a widely heterogeneous group, possibly giving rise to conflicting results between essential tremor studies.[35] In this study, we have defined a homogeneous group of essential tremor patients, with a clear diagnosis according to the criteria defined by the Tremor Investigation Group[36] and a positive effect of propranolol, a drug with level A evidence for treatment of essential tremor.[37]

4.2 METHODS

4.2.1 PARTICIPANTS

In total, 40 patients and 22 healthy controls were included. This study was conducted in two academic hospitals in The Netherlands: the Academic Medical Center in Amsterdam and the University Medical Center Groningen. Patients with a definite diagnosis of essential tremor according to criteria defined by the Tremor Investigation Group were selected if they fulfilled the following criteria:[36] bilateral upper limb tremor, an age at onset <65 years, and a disease duration >5 years. Furthermore, patients had to be right handed and report a positive effect of propranolol on the tremor. Healthy controls, matched for age, gender and handedness, were selected. Exclusion criteria were: a score <26 on the Mini-Mental State Examination, neurological disorders (for patients: other than essential tremor), age <18 years, the use of medication affecting the CNS and magnetic resonance-related contra-indications. Tremor severity was assessed OFF medication by an experienced movement disorders neurologist (J.D.S.) using the Fahn-Tolosa-Marin Tremor Rating Scale (TRS) parts A and B.[38] Medication was discontinued at least 3 days before the study. Item A on the TRS represents tremor severity of the arms in rest, posture and during action. Item B represents clinical assessment of tremor severity during tremor-inducing task performance. Finally, tremor severity was assessed using a Visual Analogue Scale (VAS). The study was approved by the local medical ethical committees and conducted according to the Declaration of Helsinki. All participants gave written informed consent.

4.2.2 FUNCTIONAL MRI TASK

A functional MRI scan was performed, while EMG was recorded simultaneously, OFF medication. Participants executed a motor task in which they were instructed to alternate 21 periods of 30 s rest with 20 periods of 30 s performing the task. Before scanning, subjects were first carefully instructed about the motor task and then practised it outside the scanner to ascertain correct task performance. Patients with essential tremor performed right hand and arm extension, the aim being to induce action tremor. Healthy controls were instructed to mimic a tremor during all task blocks by extending the right arm and performing self-paced wrist flexion-extension. As essential tremor is known to aggravate during mental tasks, an additional silent reading task was presented during half of all action blocks, with the aim to evoke more variation in tremor amplitude.[39] During the other half of action blocks, a visual task instruction 'stretch out your arm' was presented during scanning, which elicited tremor as well. All instructions were presented using slides projected onto a screen located outside the scanner bore and visible by way of a mirror. Correct task performance was assessed by visual inspection during scanning.

4.2.3 DATA ACQUISITION AND PREPROCESSING

For full details of functional MRI and EMG acquisition and preprocessing see the online Supplementary material. Images were acquired using a Philips 3 T Magnetic Resonance scanner at both sites. T_2*-weighted, 3D functional images were obtained using multislice echo planar imaging (EPI) with an echo time of 30 ms and a repetition time of 2000 ms. EMG was recorded simultaneously (BrainProducts (UMCG) and MicroMed (AMC)) from five right arm muscles. EMG data were corrected for magnetic resonance artefacts using the magnetic resonance artefact correction algorithms (Imaging Artefact Reduction method;[40] UMCG data) embedded in the BrainVision Analyzer software (BrainProducts) and FARM (functional MRI artefact reduction for motion;[41] AMC data). Functional MRI data were analysed using SPM12 (Wellcome Trust Centre for Neuroimaging, UCL, London, UK; http://www.fil.ion.ucl.ac.uk/spm, v6225, DCM version 12), and included standard preprocessing (Supplementary material). Inspection of the EMG was used to correct the block design regressor for actual onand offsets of the motor task. For each subject, scan-by-scan EMG power was calculated in a 5-Hz band around the peak tremor frequency. Finally, this EMG 'tremor' vector was orthogonalized with respect to the block regressor, scaled to the maximum value per subject to ensure that the variance was similar between subjects, convolved with the canonical haemodynamic response function and used as a regressor (residual-EMG) in the General Linear Model.[26] As motion-related and other non-neuronal signal changes are effectively reduced by global signal regression, tissue-based signals and their first derivative were also used as nuisance regressors and were calculated as the average signal across all voxels within the whole-brain mask.[42] Each single-subject first-level model thus consisted of two block regressors for the motor task, a residual-EMG regressor, six movement regressors and two global signal regressors. For the functional connectivity

analysis, the residual-EMG regressor was excluded from the first-level models as the objective of this analysis was to primarily look at the integrity of the motor network without concurrently assessing tremor severity. Brain activations during motor task execution and tremor-related (EMG-based) activations are reported elsewhere in more detail.[29] In short, motor task-related activations were found in the well-known upper-limb motor network, i.e. both for patients with essential tremor and healthy controls in motor, premotor and supplementary motor areas. In patients with essential tremor, we found tremor-related (EMG-based) activations in the left primary motor cortex (M1), supplementary motor area (SMA), premotor cortex (PMC) and thalamus, and bilaterally in the cerebellum: in left lobules VI and V, and in right lobules V, VI, and VIII, and in the brainstem. Ipsilateral cerebellar activity was related to mimicked-tremor in healthy participants. Tremor-based activations are used in the effective connectivity analysis; motor-task-based activations are used in the functional connectivity analysis. Finally, the amount of head movement during scanning was estimated by calculating the summed Euclidean distance between the first and last scan per individual subject for translation (i.e. x, y and z direction) and rotation (i.e. pitch, roll, yaw) separately, and compared between patients and healthy controls using two-sample two-tailed *t*-tests.[27]

4.2.4 EFFECTIVE CONNECTIVITY: DYNAMIC CAUSAL MODELLING

DCM models how neural activity within a network of brain regions is driven by external perturbations that result from experimentally controlled manipulations.[31] These perturbations are described by means of external inputs u that can enter the model in one of two ways.[43] First, they can elicit responses through direct influences on specific regions and can be described as 'driving' inputs or 'stimulus-bound perturbations'. An example would be the command to stretch out your arm. Second, they can change the strength of coupling among or within regions, and can be described as 'modulatory' inputs or 'contextual perturbations'. For example, fluctuations in tremor severity over time could change the intrinsic activity within regions of the cerebello-thalamo-cortical network. An important concept in DCM is that regions contain self-inhibitory properties, mediated by self-connections ('intrinsic' or within-region connections), preventing runaway outbursts of neural activity. The left M1, left PMC, left SMA, left ventral lateral nucleus of the thalamus, right cerebellar lobule V/VI and right cerebellar lobule VIII were included in our models as these regions have been associated with tremor previously using functional MRI[34,44] and showed tremor-related (EMG-based) activations in the patient group, as mentioned previously.[29] Regions were defined for each patient individually, based on activations associated with the residual-EMG regressor, and centred at the location of the local maxima with a 4mm radius, within 10mm of the group maximum (MNI coordinates: M1 x -36 y -22 z 61; PMC x -28 y -22 z 54; SMA x -2 y -14 z 55; thalamus x -12 y -24 z -1; cerebellar lobule V/VI x 34 y -50 z -25; cerebellar lobule VIII x 21 y -52 z -56). We assumed full endogenous connectivity between regions, with the exemption of connections between cerebellar regions and the thalamus (only unidirectional from cerebellum to thalamus) and between cortical and

cerebellar regions (only unidirectional from cortical to cerebellar regions) based on neuronal tracing studies in macaque monkeys (Figure 4.1),[45] leaving 28 endogenous connections. We furthermore assumed a direct effect of the motor task on the activity of all premotor regions (left SMA, left PMC).[46,47] The task regressor was divided into two separate regressors to compare the direct effects of the motor task and the motor plus silent reading task to each other. The residual EMG regressor, which represents variations in tremor amplitude over time, was included as a modulatory input on the intrinsic connections of all regions (Figure 4.2A). In this manner, the residual EMG regressor functions as a modifier of the 'state' a region is in depending on the intensity of tremor. Since the dentate nucleus is an important region within the tremor network, but not included as a node in our network, additional interest was focused on the cerebello-thalamic connections. These connections represent the net effect of the cerebello-dentatal output onto the thalamus. Therefore, modulatory input of tremor onto the cerebello-thalamic connections was added to the model space (Figure 4.1). This gave a total of 2^7=128 models. Figure 4.1 gives an overview of the DCM framework for this study; a list of models and their modulatory inputs is provided in the Supplementary material. Models were compared using Bayesian model selection (BMS) on group level.[43,48,49] Subsequently, a post hoc Bayesian model selection family analysis was used to evaluate the exceedance probabilities of a modulatory effect on each region or connection. The exceedance probability (Φ) corresponds to the belief that a model or family is more likely than any other, given the data from all subjects.[48]. We then used random effects Bayesian model averaging (BMA) on the winning half of model space, in which parameter estimates are weighted by the model evidence to compare resulting coupling parameters.[49,50] This method is convenient when many models are compared and when there is no obvious winning model. The posterior densities of the parameters are calculated across subjects and across the winning halve of models. More weight is given to the models with the highest posterior probability according to Bayes' rule.[48] The resulting coupling parameters represent connection strengths.[31]

The posterior distributions are calculated using a Gibbs sampling approach by drawing samples from a multinomial distribution of posterior beliefs for the included models.[48] Subsequently, posterior means and standard deviations of parameters were obtained and tested for significance using one-sample two-tailed *t*-tests. Because we tested 40 parameters of interest (28 endogenous, eight modulatory and four task inputs) we have adjusted the significance threshold using the Bonferroni method ($\alpha=1-(1-\alpha)^{1/40}$)=0.001282). Positive coupling parameters suggest a facilitation of neural activity, whereas negative coupling parameters can be interpreted as inhibition of neural activity. Coupling parameters are reported in Hz, reflecting the amount of activity that 'flows' from one region to another per second. For the effective connectivity analysis, we chose to include only essential tremor patients and not to include a group comparison as the two 'tasks' performed by both groups (mimicking tremor versus real tremor) are qualitatively different.

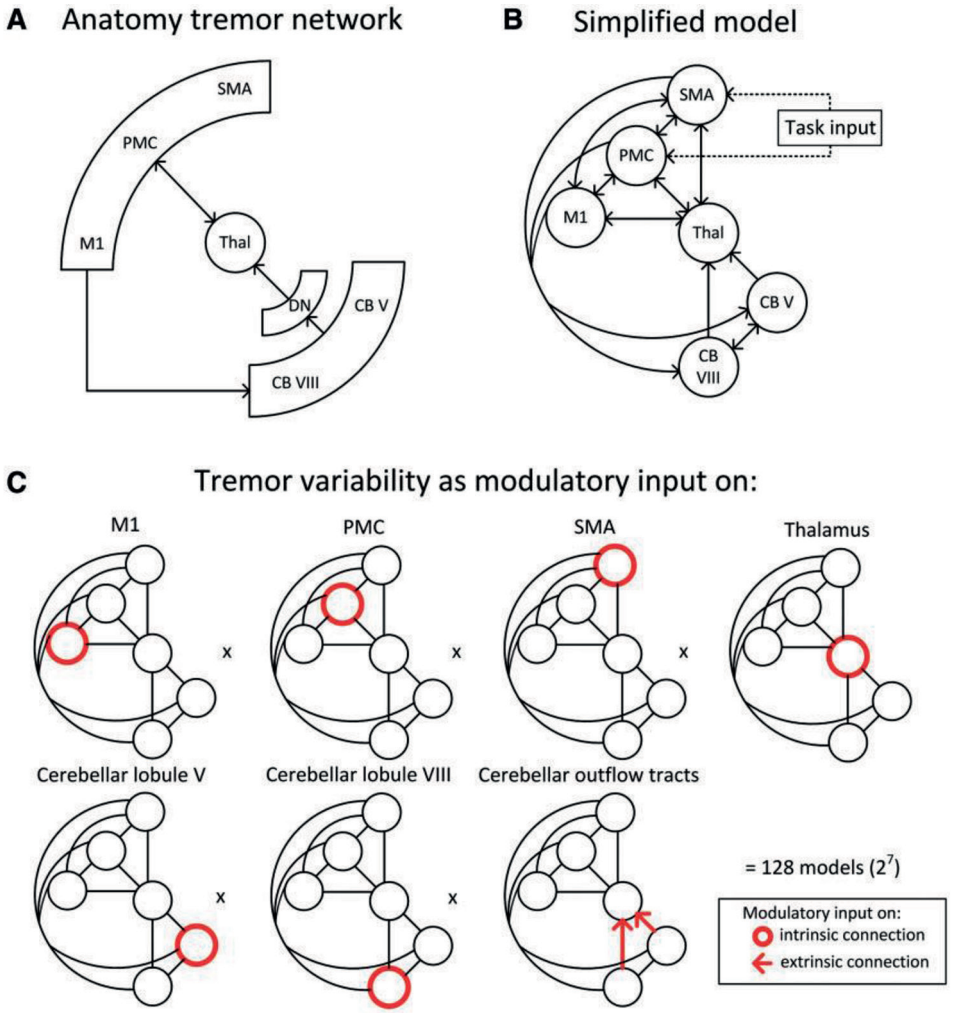

Figure 4.1 Overview of the model space. **A**: Anatomy of the tremor network as derived from Helmich et al. (2013). **B**: Simplified model derived from the anatomical tremor network to be used for the DCM analysis. Task input (the command to stretch out the arm) entered the model on SMA and PMC. **C**: The residual EMG regressor, or 'tremor variability', entered the model as modulatory input, affecting the intrinsic connections within regions and affecting the extrinsic cerebello-thalamic connections. 128 models in total were set up. CB lob V: right cerebellar lobule V; CB lob VIII: right cerebellar lobule VIII.

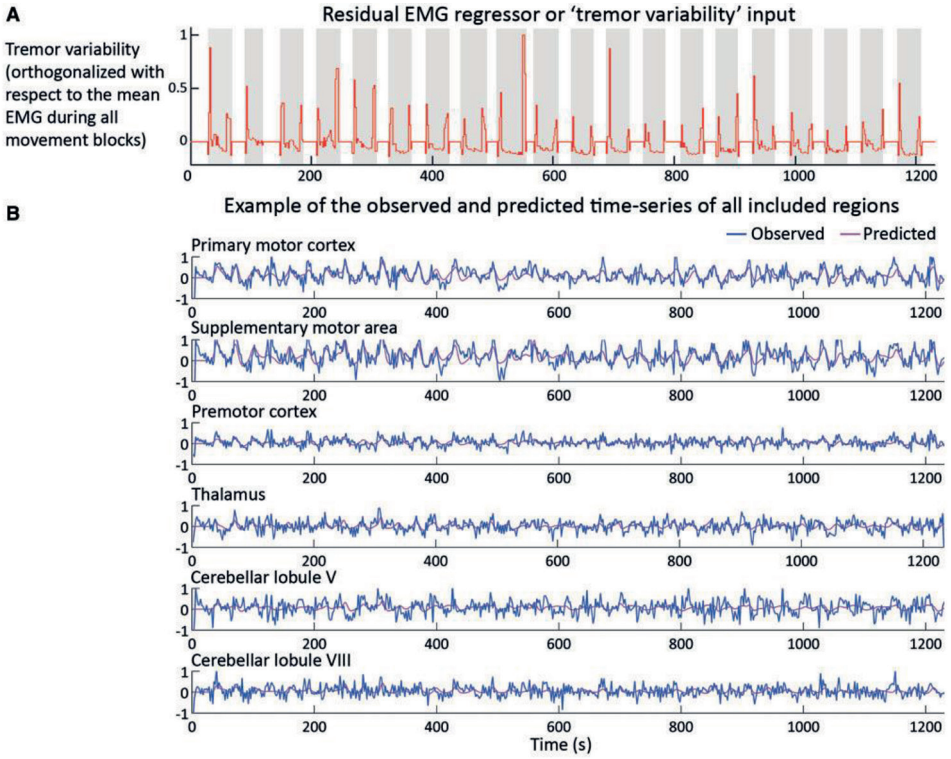

Figure 4.2 Example of the included residual EMG regressor and observed and predicted blood oxygen level-dependent time courses based on DCM. **A**: Scaled residual EMG regressor or 'tremor variability' input displayed as a function of time, representing changes in EMG power over scans of one subject. Grey bars represent the motor task during which subjects had to stretch out their arm. **B**: Example of model fit of the same subject; observed and predicted blood oxygen level-dependent time courses of all regions included in the model based on the DCM estimation. Blue: observed; purple: predicted.

4.2.5 FUNCTIONAL CONNECTIVITY: SEED-BASED CORRELATION ANALYSIS

To assess the functional integrity of the motor network in essential tremor, we performed separate seed-based functional connectivity analyses between six areas showing the strongest response relating to the motor task in essential tremor patients and healthy controls: left M1, left SMA and right cerebellar hemisphere lobules IV, V, VI and VIII (Supplementary material). We chose to look at activations related to the motor task because this allowed us to compare patients with essential tremor to healthy controls, and because functional coupling between cerebellar and cortical motor regions is most specific during motor tasks.[33] Time courses of all regions were obtained by extracting the first eigenvariates with SPM12, adjusted for effects of interest, for significant voxels using a threshold of $p<0.001$ (uncorrected).[27,33,51] Regions were defined for each subject, individually centred at the location of the local maxima with a 4-mm radius,

within 10 mm of the group maximum (MNI coordinates: M1 x -28 y -28 z 53; SMA x -2 y -8 z 57; cerebellar lobule I–IV x 4 y -64 z -21; cerebellar lobule V x 14 y -50 z -19; cerebellar lobule VI x 22 y -50 z -25; cerebellar lobule VIII x 24 y -58 z -9). For each subject and each region, we then entered this time course as a regressor in a multiple regression analysis together with the task regressor and nuisance regressors. The task regressor was added to exclude activations related to the motor task. For the second-level between group comparisons, non-parametric permutation tests were performed; this is preferred over parametric methods as this does not require that the data are normally distributed[52] (Statistical non-Parametric Mapping 13b, http://www.sph.umich.edu/ni-stat/SnPM/[53] 10 000 permutations). Contrasts were built to test (i) for significant between-group differences in functional connectivity; and (ii) for significant correlations of functional connectivity within the patient group with clinically assessed tremor severity (TRS A + B), subjectively assessed tremor severity (VAS) and disease duration. Correlations between objective (i.e. TRS A + B) and subjective (i.e. VAS) measures of tremor severity are known to be limited.[54] We expect TRS A + B to give the best representation of tremor amplitude, whereas VAS scores entail several entities such as tremor severity, psychological and social factors.[54] A cluster-wise inference was used ($p<0.05$ (FWE corrected), cluster-forming threshold $p<0.001$). To test specifically for changes in cerebellarcortical correlations, seed-based correlations were masked with either the whole cerebellum (for the M1 and SMA seed)[55] or a cerebral motor mask including left M1, left PMC, left SMA and left thalamus (for the cerebellar seeds).[56] The probabilistic atlas of the cerebellar cortex and the AAL toolbox were used to define anatomical locations of activations.[56,57]

4.3 RESULTS

4.3.1 PARTICIPANTS

Eighteen patients and one healthy control were excluded for further analysis. Reasons for exclusion of data sets were sudden excessive head movements during scanning causing striping artefacts (one patient, one healthy control), insufficient tremor during functional MRI data collection (16 patients) or failure of equipment during scanning (one patient). Healthy controls (14 male) had a median age of 56.5 years (range 20-72). For the effective connectivity analysis, four additional patients were excluded because they did not show significant tremor-related activations at an uncorrected threshold of $p<0.001$, a prerequisite for the DCM analysis, thus 18 patients were included in the effective connectivity analysis. See Table 4.1 for a full overview of included essential tremor patients. Included patients and healthy controls exhibited similar amounts of head movement during scanning (mean translation parameters: patients: 2.64 mm standard deviation (SD) 1.36; healthy controls: mean translation parameters 2.68 mm (SD 0.97), $t(42)=0.2720$, $p=0.92$; and mean rotation parameters: patients: 0.056° (SD 0.03); healthy controls 0.052° (SD 0.03), $t(42)=0.43$, $p=0.67$).

Table 4.1 Patient characteristics

	Age	Gender	Tremor frequency (Hz)	TRS A+B	Duration (years)	Family history	Propranolol use (mg)	VAS-score off medication	Alcohol sensitivity
1	21	Male	10	8	11	+	40	5.4	+
2	22	Male	7	6	10	-	20	5.2	+
3	27	Male	7.5	16	27	-	160	8.7	+
4	30	Female	8	7	15	+	20	2.9	?
5	35	Male	8	11	28	+	80	7.8	?
6	46	Male	7.5	10	41	+	80	4.4	+
7	47	Male	7	10	32	+	40	6.0	+
8	48	Female	7	27	38	+	120	5.4	-
9	53	Female	7.5	22	25	+	30	7.8	+
10	62	Female	8.5	5	57	+	100	8.5	?
11	63	Male	7	11	20	+	40	3.4	+
12	63	Female	7.5	21	24	+	80	7.4	+
13	64	Male	6.5	7	52	+	20	4.0	+
14	65	Female	7.5	4	5	+	80	2.7	?
15	69	Male	7.5	8	29	+	40	9.2	-
16	73	Female	5	21	55	+	80	2.6	+
17	74	Male	9	23	24	-	80	6.6	?
18	80	Female	6	29	20	+	80	6.9	+
Excluded from the effective connectivity analysis:									
19	32	Female	7	10	29	+	40	6.0	?
20	53	Male	8	15	37	+	50	8.6	+
21	57	Female	7	17	40	+	10	4.0	?
22	72	Male	6	31	62	+	320	9.2	+
Median (range)	59.5 (21-80)	M: 12 F: 10	7.5 (5-10)	11 (4-31)	30.5 (5-62)	+: 19 -: 3	65 (20-320)	6.0 (2.6 – 9.2)	+: 13 -: 2 ?: 7

Four patients were excluded for the effective connectivity analysis due to absent significant tremor-related activations at an uncorrected threshold of $p<0.001$. VAS: range 0–10. TRS A + B scores were assessed while OFF medication. + = positive; -= negative; ? = unknown.

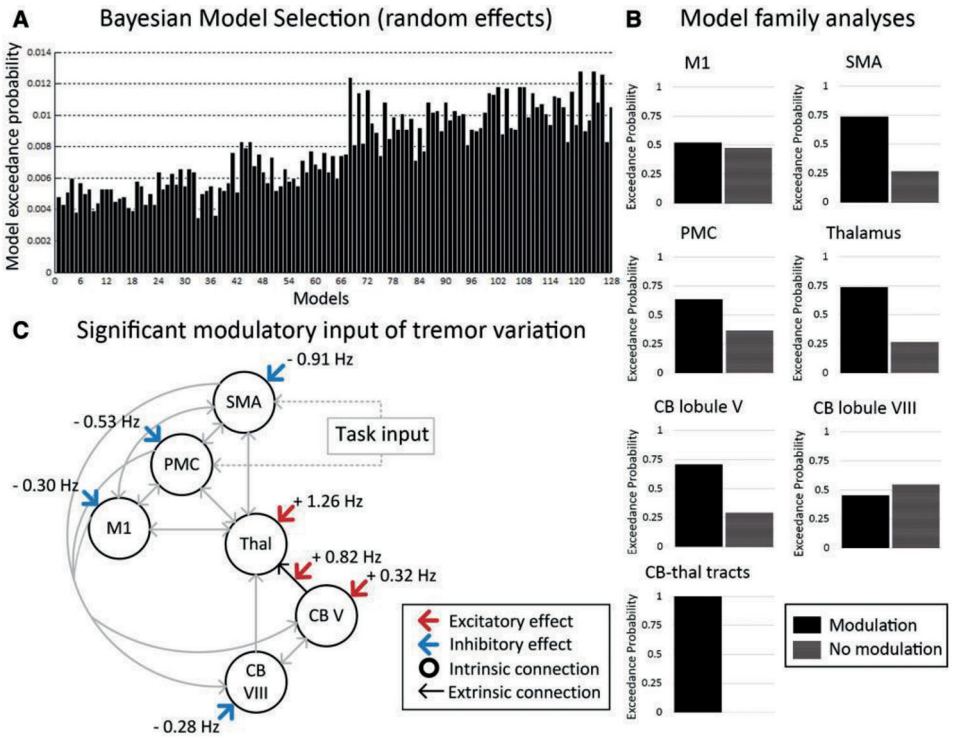

Figure 4.3 Results of Bayesian model selection and Bayesian model averaging in essential tremor patients. **A**: Exceedance probabilities of all 128 models. Models 1-64 have no modulatory input on the cerebello-thalamic connections, Models 65-128 have modulatory input on the cerebello-thalamic connections. **B**: Post hoc family analysis identified a preference for models with a modulatory effect on the cerebellar-thalamic connections (Φ>99%). **C**: Graphical representation of the significant estimated connectivity parameters resulting from Bayesian Model Averaging in essential tremor. For clarity reasons only modulatory influences are depicted. Coupling parameter strength is depicted in red (excitatory effect) and blue (inhibitory effect). Significant modulatory input is depicted in Hz. Thal: left thalamus; CB lob V: right cerebellar lobule V; CB lob VIII: right cerebellar lobule VIII. For full coupling parameter details see Supplementary material.

4.3.2 EFFECTIVE CONNECTIVITY: BAYESIAN MODEL SELECTION

Figure 4.2B gives an example of observed and predicted blood oxygen level-dependent time courses of one subject, based on the DCM estimation. Model 124 showed the highest posterior exceedance probability (Φ=0.0128), but is closely followed by several other models. Based on the Bayesian model selection there was no obvious winning model (Figure 4.3A). The post hoc family analysis, where models are grouped by the presence of modulatory effects on the six tremor regions and cerebello-dentato-thalamic pathway, showed quite convincingly that modulatory input on the cerebello-thalamic connections (Φ>99) was more likely than no input

on the cerebello-thalamic connections (Figure 4.3B). The thalamus (Φ=0.74), cerebellar lobule V (Φ=0.71), SMA (Φ=0.74) and PMC (Φ=0.63) were also more likely to be modulated by tremor variation (Figure 4.3B). The primary motor cortex (Φ=0.52) and cerebellar lobule VIII (Φ=0.45) showed no clear preference for models with or without modulatory input of tremor variation.

4.3.3 EFFECTIVE CONNECTIVITY: BAYESIAN MODEL AVERAGING

Modulatory inputs on the six intrinsic and two extrinsic, cerebello-dentato-thalamic, connections were extracted. Modulatory input of tremor variation exhibited a significant excitatory influence on the intrinsic thalamic (mean 1.26, SD 0.42, $p<0.0000$) and cerebellar lobule V (mean 0.32, SD 0.32, $p=0.0006$) connections, and on the extrinsic connection from cerebellar lobule V to the thalamus (mean 0.82, SD 0.89, $p=0.00128$). Modulatory input of tremor variation exhibited a significant inhibitory influence on M1 (mean -0.30, SD 0.25, $p<0.0000$), SMA (mean -0.91, SD 0.27, $p<0.0000$), PMC (mean -0.55, SD 0.29, $p<0.0000$) and cerebellar lobule VIII (mean -0.28, SD 0.27, $p=0.0003$). Results are summarized in Figure 4.3C. There was a significant driving force of task on SMA and PMC (see Supplementary material for full details of endogenous and driving coupling parameters).

Furthermore, there was a difference in driving force on the SMA between the motor task with reading versus without reading ($t(34)=10.79$, $p<0.0000$). There was no difference in driving force between tasks on the PMC ($t(34)=0.13$, $p=0.39$).

4.3.4 FUNCTIONAL CONNECTIVITY RESULTS IN ESSENTIAL TREMOR AND HEALTHY CONTROLS

In essential tremor patients, the M1 and SMA seeds showed reduced functional connectivity with right cerebellar lobules V and VI compared to healthy controls (Figure 4.4A and Table 4.2). Right cerebellar lobules I–IV, V, VI and VIII seeds all showed reduced functional connectivity with M1 and SMA compared to healthy controls (Table 4.2). For the M1 seed, functional connectivity with right cerebellar lobules VI, crus II, vermis VI and lobule VIII, and left cerebellar lobule VIIb, crus II and lobule VIII, correlated negatively with tremor severity (TRS A + B). For the cerebellar lobule VIII seed, functional connectivity with the primary motor cortex correlated negatively with tremor severity (TRS A + B) (Figure 4.4B and Table 4.3). M1 and cerebellar lobule VIII thus show a reciprocally observed functional disconnection correlated to increasing tremor severity. For the right cerebellar lobule I–IV seed, functional connectivity with the left thalamus correlated positively with tremor severity (TRS A + B) (Figure 4.4B and Table 4.3). None of the seed regions' functional connectivities correlated with VAS scores or disease duration.

Table 4.2 Local maxima of group differences in cerebello-cortical functional connectivity

Region	Hemisphere	*t*-value	$P_{FWE\text{-}corr}$	Cluster size	x (mm)	y (mm)	z (mm)
Controls > ET – left M1 seed							
Cerebellar lobule V	Right	4.68	0.0078	86	14	-50	-13
Cerebellar lobule V	Right	3.95			22	-46	-23
Cerebellar lobule VI	Right	3.93			18	-54	-21
Cerebellar lobule VI	Right	4.36	0.0231	43	30	-64	-27
Controls > ET – left SMA seed							
Cerebellar vermis VI	Right	4.49	0.0366	29	2	-62	-27
Cerebellar lobule VI	Right	4.41	0.0049	128	24	-50	-25
Cerebellar lobule V	Right	4.24			16	-46	-25
Cerebellar lobule V	Right	4.40	0.0079	102	12	-48	-13
Cerebellar lobule V	Right	4.03			12	-60	-13
Cerebellar lobule VI	Left	4.35	0.0269	38	-12	-74	-25
Controls > ET – right cerebellar lobule IV seed							
Primary motor cortex	Left	6.46	0.0035	85	-32	-22	49
Supplementary motor area	Left	4.33	0.0381	24	-2	2	59
Controls > ET – right cerebellar lobule V seed							
Supplementary motor area	Left	4.89	0.0287	26	0	4	61
Primary motor cortex	Left	4.68	0.0160	34	-32	22	45
Controls > ET – right cerebellar lobule VI seed							
Primary motor cortex	Left	5.59	0.0088	49	-34	-24	49
Supplementary motor area	Left	4.92	0.0042	72	-2	2	61
Supplementary motor area	Left	3.81			0	4	51
Primary motor cortex	Left	4.58	0.0234	29	-44	-4	49
Controls > ET – right cerebellar lobule VIII seed							
Supplementary motor area	Left	4.02	0.0301	27	-2	2	59
Supplementary motor area	Left	3.68			0	10	55
Primary motor cortex	Left	3.80	0.0383	23	-50	-5	51
Primary motor cortex	Left	3.67			-44	-2	53

Stereotactic coordinates of local maxima of cerebello-cortical functional connectivity in essential tremor patients compared to controls ($p>0.05$, FWE corrected, cluster-defining threshold of $p<0.001$), coordinates in MNI space. ET: essential tremor.

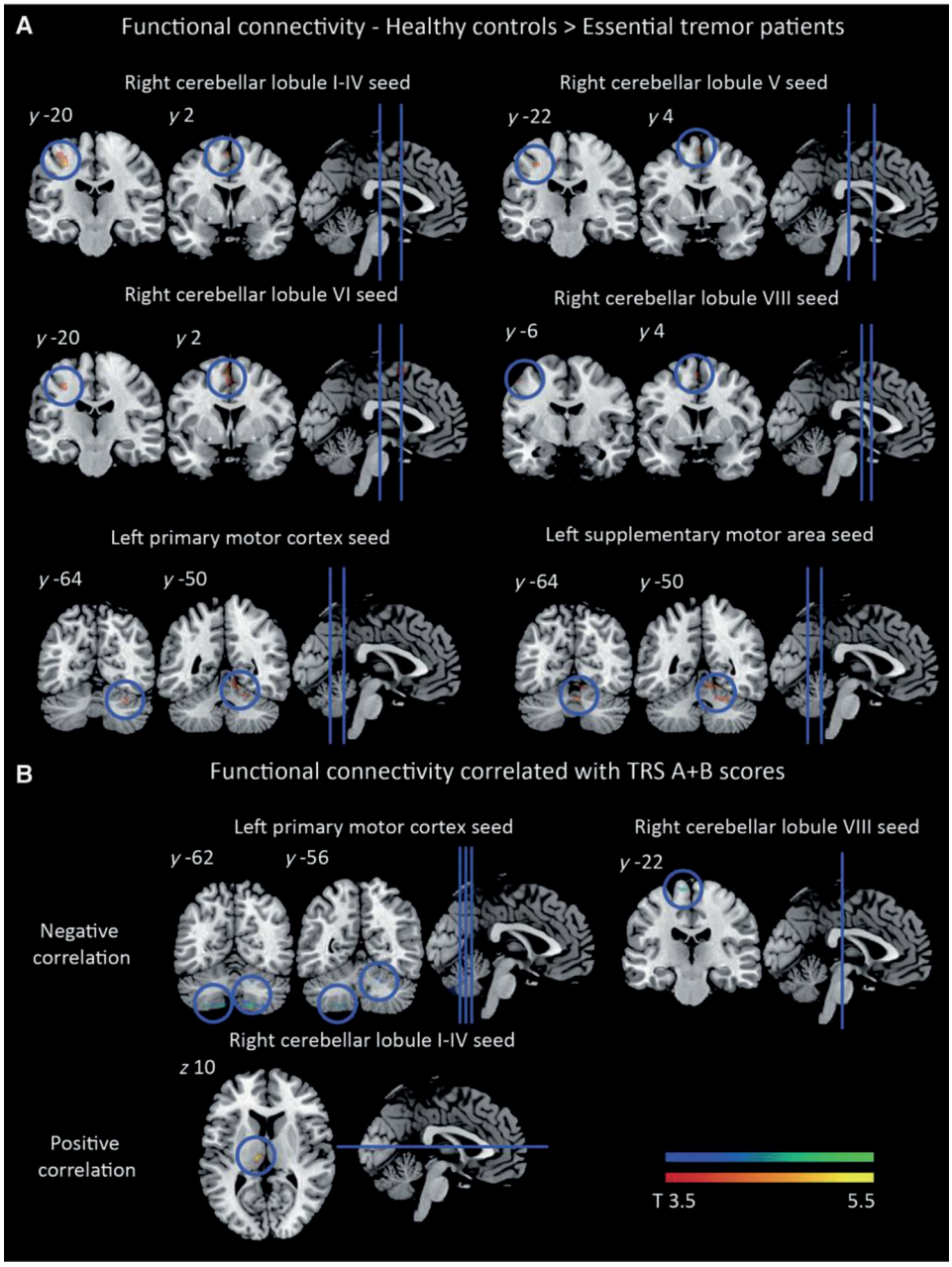

Figure 4.4 Decreased cerebellar-cortical functional connectivity in essential tremor. A: Between-group differences illustrating areas of decreased connectivity in patients with essential tremor compared to healthy controls for the M1, SMA, cerebellar lobule I–IV, V, VI and VIII seeds. **B**: Correlation between connectivity and TRS A + B scores for the M1, cerebellar lobule I–IV and VIII seed. Results are projected on the ch2better-template using MRIcroN. Cluster-wise inference is used ($p<0.05$ FWE corrected, cluster-defining threshold of $p<0.001$).

Table 4.3 Local maxima of cerebello-cortical functional connectivity correlated with tremor severity

Region	Hemisphere	*t*-value	$P_{FWE\text{-}corr}$	Cluster size	x (mm)	y (mm)	z (mm)
ET correlated negatively with TRS A + B – left M1 seed							
Cerebellar lobule crus II	Left	5.98	0.0003	645	-28	-78	-51
Cerebellar lobule VIIb	Left	5.29			-6	-74	-39
Cerebellar lobule crus II	Right	5.09			4	-80	-35
Cerebellar vermis VI		4.51	0.0298	38	0	-70	-23
Cerebellar lobule VI	Right				10	-72	-29
Cerebellar lobule VI	Right	4.38	0.0338	34	18	-56	-27
ET correlated negatively with TRS A + B – right cerebellar lobule VIII seed							
Primary motor cortex	Left	5.37	0.0143	31	-6	-22	73
Primary motor cortex	Left	4.66			-4	-14	71
ET correlated positively with TRS A + B – right cerebellar vermis seed							
Thalamus	Left	5.40	0.0429	23	-10	-20	11
Thalamus		3.78			-10	-28	9

Stereotactic coordinates of local maxima of cerebello-cortical functional connectivity in essential tremor patients correlated with tremor severity ($p>0.05$, FWE corrected, cluster defining threshold of $p<0.001$), coordinates in MNI space. ET: essential tremor.

4.4 DISCUSSION

This study provides two novel findings that support an important role for the cerebellum, the thalamus, and the cerebello-dentato-thalamic tracts in the pathophysiology of essential tremor. First, the effective connectivity analysis demonstrated a significant excitatory modulating effect of tremor variation on the extrinsic cerebello-dentato-thalamic connection and on intrinsic thalamic and cerebellar lobule V activity. Furthermore, we have replicated and expanded findings of decreased cerebello-cortical functional connectivity, related to a motor task, between the motor cerebellum and cortical motor areas in essential tremor patients compared to controls.[34] More importantly, decreased functional coupling between the primary motor cortex and posterior cerebellum was associated with an increase in clinically assessed tremor severity during the motor task. Additionally, an increase in clinically assessed tremor severity was associated with increased functional connectivity between cerebellar lobule I–IV and the motor thalamus in patients with essential tremor.

4.4.1 ALTERED CEREBELLAR OUTPUT

Our findings advocate that modulatory tremor input is associated with activity within the cerebello-dentatothalamic network. During the motor task, inducing action tremor, all included motor regions exhibited self-inhibiting properties. When incorporating tremor variation during the motor task, intrinsic inhibitory activity of the cortical motor regions and cerebellar

lobule VIII increased. However, tremor modulation exhibited an excitatory modulating effect on the cerebello-dentato-thalamic tract, leading from cerebellar lobule V to the thalamus, and intrinsic cerebellar lobule V and thalamic activity. Our results do not give a direct answer as to whether this excitation would give rise to tremor. It is important to note that this excitation does not directly represent a neurophysiological correlate, but is modelled based on the functional MRI and EMG signals. Our results do indicate that cerebello-dentato-thalamic activity is perturbed in essential tremor, which can be placed in a broader framework of evidence regarding the pathophysiology of essential tremor. Previously, GABAergic neurotransmission dysfunction within the cerebellum has been observed, with increased 11C-flunazenil binding to GABA-receptors in the cerebellar cortex, increasing with tremor severity.[58] Pathology studies also show evidence for cerebellar changes, with Purkinje cell loss and axonal swelling,[17,18,59] and simultaneous remodelling of the cerebellar cortex.[19,20,60] Purkinje cells from the sole output channel from the cerebellar cortex, and lead to the deep cerebellar nuclei, including the dentate nucleus. GABAergic Purkinje cell synapses constitute the majority of all synapses in the dentate nucleus, with their action strongly regulating the intrinsic activity of the dentate nucleus.[61] Besides pathological changes in the cerebellar cortex, altered dentate nucleus function has been postulated in essential tremor.[6,21,62] Whether the cerebellar cortical pathology is secondary to changes in the dentate nucleus, or vice versa, remains controversial. Altered 11C-flunazenil binding to GABA-receptors[62] and a decrease in the number of GABA receptors in the dentate nucleus in essential tremor patients[21] both suggest abnormal functionality of GABA receptors within the dentate nucleus. Electrophysiology data indicate that neurons within the dentate nucleus possess a pacemaker-like activity, with the ability to generate spontaneous inhibitory postsynaptic potentials, which can be increased or decreased depending on GABAergic Purkinje cell input.[63] Tremor could consequently result from a disinhibited dentate nucleus and subsequent pathological entrainment of the cerebello-thalamo-cortical network.[64] This may be explained as a result of loss of GABAergic tone in the cerebellar system (Figure 4.5). A recent functional MRI study using a finger-tapping task showed increased activity of the dentate nucleus with increasing clinical tremor severity, in line with this hypothesis.[6]

4.4.2 FUNCTIONAL INTEGRITY OF THE MOTOR NETWORK

Patients with essential tremor demonstrate decreased functional coupling between cerebellar motor areas and cortical motor areas compared to controls during a motor task. Furthermore, a decrease in functional coupling between the primary motor cortex and posterior cerebellum is correlated with an increase in tremor severity. Two recent functional MRI studies using a motor task showed decreased activity of cerebellar motor regions related to a motor task in essential tremor.[6,34] Our results support the hypothesis that increasing tremor severity proportionally disrupts cerebello-cortical connectivity. Moreover, continuous increased input from the dentate nucleus via the thalamus could cause amplification of inhibitory mechanisms within the cerebral cortex. Inhibitory circuits within the motor cortex are reported to be aberrant and

less modifiable in essential tremor.[66] In addition, increased 11C-flunazenil binding to GABA-receptors has also been found in the ventrolateral thalamus and lateral premotor cortex in essential tremor.[62]

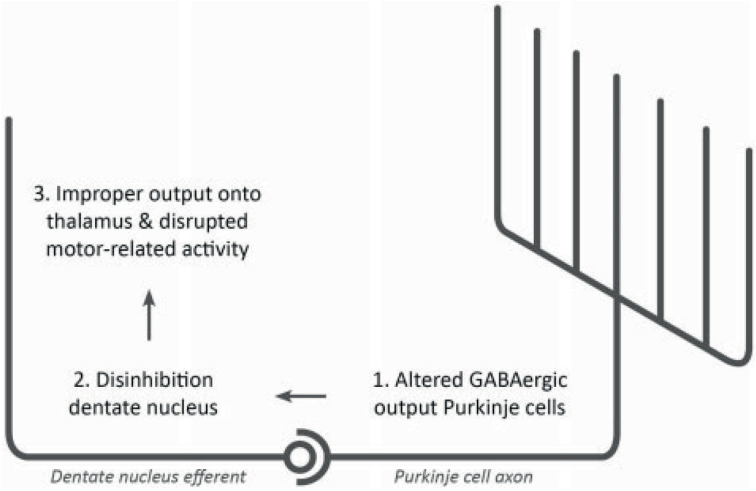

Figure 4.5 Hypothetical chain of pathological events inducing tremor. First, neurodegeneration and neurotransmission dysfunction within the cerebellar cortex lead to altered GABAergic cerebellar cortical output. Second, this causes disinhibition of the dentate nucleus, altering its pacemaker-like activity. Consequently and third, pathological activity is passed onward towards the thalamus through dentate nucleus efferents, disrupting physiological motor-related connectivity within the cortex.

4.4.3 DIFFERENTIAL INVOLVEMENT OF THE ANTERIOR AND POSTERIOR CEREBELLUM IN ESSENTIAL TREMOR

The anterior cerebellum is formed by lobules I to V/VI, and is divided by the primary fissure from the posterior cerebellum, formed by lobules VI/VII to X.[67,68] Interestingly, to our knowledge, the anterior and posterior cerebellum, although both involved in motor control, are not discussed separately in essential tremor research, even though the physiological, developmental and genetic properties of each are quite different.[67-69] Our functional and effective connectivity results suggest that both the anterior and posterior cerebellum are involved in essential tremor. There is, however, a discrepancy in reduced functional connectivity between M1 and the posterior cerebellum associated with increasing tremor severity, and an apparent lack of this reduced functional connectivity between M1 and regions within the anterior cerebellum. On the other hand, an excitatory modulatory effect of tremor was observed in cerebellar lobule V (anterior cerebellum) and on the connections between cerebellar lobule V and the thalamus. We currently have no clear explanation for this observed difference. Although this discrepancy

could be due to insufficient sample size, for future pathology studies, it would be of interest to divorce the involvements of the anterior and posterior cerebellum by assessing them separately.

4.4.4 METHODOLOGICAL CONSIDERATIONS

A known and persistent problem with functional MRI studies is their limited temporal resolution. This makes the identification of a tremor generator challenging. However, it is a useful technique for studying properties of regions within the cerebello-thalamo-cortical network, especially when combined with EMG recordings. This is the first time EMG signals were incorporated in a DCM analysis. It needs to be stressed that the residual EMG regressor is not the EMG signal as recorded from the muscle. It is a reflection of the waxing and waning EMG signal with respect to the task, i.e. the involuntary movements, and does not necessarily say something about clinical severity. Further studies using electrophysiological techniques may be required to provide deeper insights into the synaptic mechanisms involved. Although our results appear robust, they will need to be replicated in the future. For this study, the parameters characterizing the cerebello-thalamic connections were chosen as indirect measures to assess the possible involvement of the dentate nucleus and the cerebellodentato-thalamic tract in essential tremor. These connections represent the net effect of the cerebello-dentato-thalamic tracts. No tremor-related activity was observed in the dentate nucleus in individual subjects, possibly due to the high iron-content of the dentate nucleus and resulting low signal-to-noise ratio of its blood oxygen level-dependent signal.[70] To be able to include the dentate nucleus in future models, studies with a higher spatial and temporal resolution are warranted to reproduce our observed excitatory effect on the cerebellodentato-thalamic pathway. A common difficulty in functional imaging studies lies in selecting a suitable task for healthy controls that corresponds well with the patients' task. For this study, a mimicked tremor was chosen. Consequently, the two groups were actually performing a qualitatively different task. These tasks were chosen to allow optimal distinction of brain networks for the functional connectivity analysis, involved in involuntary tremor as opposed to compensation or afferent feedback by deliberate, mimicked tremor movements. However, due to this qualitative difference, for the effective connectivity analysis the patient group was not compared with a healthy control group. Future studies could circumvent this problem by using other techniques such as enforcing passive wrist oscillations as an additional control condition, as has been used previously by Bucher and colleagues (1997).[44] One could then additionally assess whether there are differences within the tremor circuitry in excitatory and inhibitory connections between patients and healthy controls. Finally, as mentioned in the 'Materials and methods' section, a silent reading task was offered during half of the task blocks, which may have influenced activity within the motor network and could therefore have affected our effective connectivity results. There was a significant difference in driving effect of the two tasks on the SMA and not on the PMC, as observed in the effective connectivity analysis. However, the motor task with silent reading had merely an additional excitatory effect compared to the motor task in which only the command to stretch

the right arm was given. We expect that this will not have affected the final conclusions of the effective connectivity analysis.

4.5 CONCLUSION

In conclusion, our findings suggest that cerebello-dentatothalamic activity and cerebellar-cortical connectivity are perturbed in essential tremor, supporting previous evidence of cerebellar pathology in essential tremor. This perturbed cerebello-dentato-thalamic activity could subsequently affect the rest of the cerebello-thalamo-cortical network, leading to tremor on the one hand and possibly less effective physiological output on the other hand. Investigating effective connectivity changes in essential tremor represents a new avenue of study that may shed light on its underlying pathophysiology.

ACKNOWLEDGEMENTS

We are grateful to all study participants for their contributions, to Aart Nederveen for support, to Alexander Munts for help with the inclusion of patients and to Marina Tijssen for her valuable comments. We thank Louise Marshall for grammatical corrections.

FUNDING

This study was funded by the Prinses Beatrix Fonds (W.OR10-01) and the Hersenstichting Nederland (2012(1)-91).

REFERENCES

1. Louis ED, Ferreira JJ. How common is the most common adult movement disorder? Update on the worldwide prevalence of essential tremor. Mov Disord. 2010;25(5):534-541. doi:10.1002/mds.22838.
2. Dupuis MJ, Evrard FL, Jacquerye PG, Picard GR, Lermen OG. Disappearance of essential tremor after stroke. Mov Disord. 2010;25(16):2884-2887. doi:10.1002/mds.23328 (doi).
3. Raethjen J, Deuschl G. The oscillating central network of Essential tremor. Clin Neurophysiol. 2012;123(1): 61-64. doi:10.1016/j.clinph.2011.09.024 (doi).
4. Passamonti L, Novellino F, Cerasa A, et al. Altered cortical-cerebellar circuits during verbal working memory in essential tremor. Brain. 2011;134(8):2274-2286. doi:10.1093/brain/awr164.
5. Grimaldi G, Manto M. Is essential tremor a purkinjopathy? The role of the cerebellar cortex in its pathogenesis. Mov Disord. 2013;28(13):1759-1761. doi:10.1002/mds.25645.
6. Buijink AWG, Broersma M, van der Stouwe AMM, et al. Rhythmic finger tapping reveals cerebellar dysfunction in essential tremor. Parkinsonism Relat Disord. 2015;21(4):383-388. doi:10.1016/j.parkreldis.2015.02.003.
7. Haubenberger D, McCrossin G, Lungu C, et al. Octanoic acid in alcohol-responsive essential tremor: A randomized controlled study. Neurology. 2013;80(10):933-940. doi:10.1212/WNL.0b013e3182840c4f.
8. Stolze H. The gait disorder of advanced essential tremor. Brain. 2001;124(11):2278-2286. doi:10.1093/brain/124.11.2278.
9. Fasano A, Herzog J, Raethjen J, et al. Gait ataxia in essential tremor is differentially modulated by thalamic stimulation. Brain. 2010;133(12):3635-3648. doi:10.1093/brain/awq267.
10. Hoskovcová M, Ulmanová O, Šprdlík O, et al. Disorders of balance and gait in essential tremor are associated with midline tremor and age. Cerebellum. 2013;12(1):27-34. doi:10.1007/s12311-012-0384-4.
11. Helmchen C, Hagenow A, Miesner J, et al. Eye movement abnormalities in essential tremor may indicate cerebellar dysfunction. Brain. 2003;126(6):1319-1332. doi:10.1093/brain/awg132.
12. Kronenbuerger M, Gerwig M, Brol B, Block F, Timmann D. Eyeblink conditioning is impaired in subjects with essential tremor. Brain. 2007;130(6):1538-1551. doi:10.1093/brain/awm081.
13. Gitchel GT, Wetzel P a, Baron MS. Slowed saccades and increased square wave jerks in essential tremor. Tremor Other Hyperkinet Mov (N Y). 2013;3:1-7. doi:10.1001/archneurol.2012.70.
14. Deuschl G, Wenzelburger R, Loffler K, Raethjen J, Stolze H. Essential tremor and cerebellar dysfunction clinical and kinematic analysis of intention tremor. Brain. 2000;123 (Pt 8(Pt 8):1568-1580.
15. Louis ED, Frucht SJ, Rios E. Intention tremor in essential tremor: Prevalence and association with disease duration. Mov Disord. 2009;24(4):626-627. doi:10.1002/mds.22370 (doi).
16. Louis ED. Re-thinking the biology of essential tremor: from models to morphology. Parkinsonism Relat Disord. 2014;20 Suppl 1:S88-93. doi:10.1016/S1353-8020(13)70023-3 (doi).
17. Louis ED, Faust PL, Vonsattel JP, et al. Neuropathological changes in essential tremor: 33 cases compared with 21 controls. Brain. 2007;130(Pt 12):3297-3307. doi:awm266 (pii).
18. Rajput AH, Robinson CA, Rajput ML, Robinson SL, Rajput A. Essential tremor is not dependent upon cerebellar Purkinje cell loss. Parkinsonism Relat Disord. 2012;18(5):626-628. doi:10.1016/j.parkreldis.2012.01.013 (doi).
19. Babij R, Lee M, Cortes E, Vonsattel JP, Faust PL, Louis ED. Purkinje cell axonal anatomy: quantifying morphometric changes in essential tremor versus control brains. Brain. 2013;136(Pt 10):3051-3061. doi:10.1093/brain/awt238 (doi).
20. Lin CY, Louis ED, Faust PL, Koeppen AH, Vonsattel JP, Kuo SH. Abnormal climbing fibre-Purkinje cell synaptic connections in the essential tremor cerebellum. Brain. 2014;137(Pt 12):3149-3159. doi:10.1093/brain/awu281 (doi).
21. Paris-Robidas S, Brochu E, Sintes M, et al. Defective dentate nucleus GABA receptors in essential tremor. Brain. 2012;135(1):105-116. doi:10.1093/brain/awr301.

22. Sharifi S, Nederveen AJ, Booij J, van Rootselaar AF. Neuroimaging essentials in essential tremor: A systematic review. NeuroImageClinical. 2014;5:217-231. doi:10.1016/j.nicl.2014.05.003 (doi).
23. Schnitzler A, Münks C, Butz M, Timmermann L, Gross J. Synchronized brain network associated with essential tremor as revealed by magnetoencephalography. Mov Disord. 2009;24(11):1629-1635. doi:10.1002/mds.22633.
24. Muthuraman M, Heute U, Arning K, et al. Oscillating central motor networks in pathological tremors and voluntary movements. What makes the difference? Neuroimage. 2012;60(2):1331-1339. doi:10.1016/j.neuroimage.2012.01.088.
25. Van Rootselaar AF, Maurits NM, Renken R, et al. Simultaneous EMG-functional MRI recordings can directly relate hyperkinetic movements to brain activity. Hum Brain Mapp. 2008;29(12):1430-1441. doi:10.1002/hbm.20477.
26. Van Rootselaar AF, Renken R, De Jong BM, Hoogduin JM, Tijssen M a J, Maurits NM. fMRI analysis for motor paradigms using EMG-based designs: A validation study. Hum Brain Mapp. 2007;28(11):1117-1127. doi:10.1002/hbm.20336.
27. Helmich RC, Janssen MJR, Oyen WJG, Bloem BR, Toni I. Pallidal dysfunction drives a cerebellothalamic circuit into Parkinson tremor. Ann Neurol. 2011;69(2):269-281. doi:10.1002/ana.22361.
28. Contarino MF, Groot PF, van der Meer JN, et al. Is there a role for combined EMG-fMRI in exploring the pathophysiology of essential tremor and improving functional neurosurgery? PLoS One. 2012;7(10):e46234. doi:10.1371/journal.pone.0046234 (doi).
29. Broersma M, Van Der Stouwe AMM, Buijink AWG, et al. Bilateral cerebellar activation in unilaterally challenged essential tremor. NeuroImage Clin. 2016;11:1-9. doi:10.1016/j.nicl.2015.12.011.
30. Friston KJ. Functional and effective connectivity in neuroimaging: A synthesis. Hum Brain Mapp. 1994;2(1-2):56-78. doi:10.1002/hbm.460020107.
31. Friston KJ, Harrison L, Penny W. Dynamic causal modelling. Neuroimage. 2003;19(4):1273-1302. doi:10.1016/S1053-8119(03)00202-7.
32. David O, Guillemain I, Saillet S, et al. Identifying neural drivers with functional MRI: an electrophysiological validation. PLoS Biol. 2008;6(12):2683-2697. doi:10.1371/journal.pbio.0060315.
33. Buckner RL, Krienen FM, Castellanos A, Diaz JC, Yeo BT. The organization of the human cerebellum estimated by intrinsic functional connectivity. J Neurophysiol. 2011;106(5):2322-2345. doi:10.1152/jn.00339.2011 (doi).
34. Neely K a, Kurani AS, Shukla P, et al. Functional Brain Activity Relates to 0-3 and 3-8 Hz Force Oscillations in Essential Tremor. Cereb Cortex. 2014. doi:10.1093/cercor/bhu142.
35. Louis ED. Essential tremors: a family of neurodegenerative disorders? Arch Neurol. 2009;66(10):1202-1208. doi:10.1001/archneurol.2009.217.
36. Bain P, Brin M, Deuschl G, et al. Criteria for the diagnosis of essential tremor. Neurology. 2000;54(11 Suppl 4):S7.
37. Deuschl G, Raethjen J, Hellriegel H, Elble R. Treatment of patients with essential tremor. Lancet Neurol. 2011;10(2):148-161. doi:10.1016/S1474-4422(10)70322-7.
38. Fahn S. Clinical Rating Scale for Tremor. Park Dis Mov Disord. 1993:271-280.
39. Koller WC, Biary NM. Volitional control of involuntary movements. Mov Disord. 1989;4(2):153-156. doi:10.1002/mds.870040207.
40. Allen PJ, Josephs O, Turner R. A method for removing imaging artifact from continuous EEG recorded during functional MRI. Neuroimage. 2000;12(2):230-239. doi:10.1006/nimg.2000.0599.
41. van der Meer JN, Tijssen MA, Bour LJ, van Rootselaar AF, Nederveen AJ. Robust EMG-fMRI artifact reduction for motion (FARM). Clin Neurophysiol. 2010;121(5):766-776. doi:10.1016/j.clinph.2009.12.035 (doi).
42. Power JD, Mitra A, Laumann TO, Snyder AZ, Schlaggar BL, Petersen SE. Methods to detect, characterize, and remove motion artifact in resting state fMRI. Neuroimage. 2014;84:320-341. doi:10.1016/j.neuroimage.2013.08.048.

43. Rigoux L, Stephan KE, Friston KJ, Daunizeau J. Bayesian model selection for group studies - revisited. Neuroimage. 2013. doi:10.1016/j.neuroimage.2013.08.065.

44. Bucher S, Seelos K, Dodel R. Activation mapping in essential tremor with functional magnetic resonance imaging. Ann Neurol. 1997:32-40. http://onlinelibrary.wiley.com/doi/10.1002/ana.410410108/full.

45. Middleton FA, Strick PL. Basal ganglia and cerebellar loops: Motor and cognitive circuits. In: Brain Research Reviews. Vol 31. ; 2000:236-250. doi:10.1016/S0165-0173(99)00040-5.

46. Goldman-Rakic PS, Bates JF, Chafee M V. The prefrontal cortex and internally generated motor acts. Curr Opin Neurobiol. 1992;2(6):830-835. doi:10.1016/0959-4388(92)90141-7.

47. Wang LE, Fink GR, Diekhoff S, Rehme AK, Eickhoff SB, Grefkes C. Noradrenergic enhancement improves motor network connectivity in stroke patients. Ann Neurol. 2011;69(2):375-388. doi:10.1002/ana.22237.

48. Penny WD, Stephan KE, Daunizeau J, et al. Comparing families of dynamic causal models. PLoS Comput Biol. 2010;6(3). doi:10.1371/journal.pcbi.1000709.

49. Stephan KE, Penny WD, Moran RJ, den Ouden HEM, Daunizeau J, Friston KJ. Ten simple rules for dynamic causal modeling. Neuroimage. 2010;49(4):3099-3109. doi:10.1016/j.neuroimage.2009.11.015.

50. Torrisi SJ, Lieberman MD, Bookheimer SY, Altshuler LL. Advancing understanding of affect labeling with dynamic causal modeling. Neuroimage. 2013;82:481-488. doi:10.1016/j.neuroimage.2013.06.025.

51. Friston KJ, Rotshtein P, Geng JJ, Sterzer P, Henson RN. A critique of functional localisers. Neuroimage. 2006;30(4):1077-1087. doi:10.1016/j.neuroimage.2005.08.012.

52. Thirion B, Pinel P, Mériaux S, Roche A, Dehaene S, Poline JB. Analysis of a large fMRI cohort: Statistical and methodological issues for group analyses. Neuroimage. 2007;35(1):105-120. doi:10.1016/j.neuroimage.2006.11.054.

53. Holmes AP, Blair RC, Watson JD, Ford I. Nonparametric analysis of statistic images from functional mapping experiments. J Cereb Blood Flow Metab. 1996;16(1):7-22. doi:10.1097/00004647-199601000-00002.

54. van der Stouwe AMM, Broersma M, Buijink AWG, van Rootselaar AF, Maurits NM. Limited correlations between clinician-based and patient-based measures of essential tremor severity. Park Relat Disord. 2015;21(6):654-657. doi:10.1016/j.parkreldis.2015.03.004.

55. Diedrichsen J. A spatially unbiased atlas template of the human cerebellum. Neuroimage. 2006;33(1):127-138. doi:S1053-8119(06)00641-0 (pii).

56. Eickhoff SB, Stephan KE, Mohlberg H, et al. A new SPM toolbox for combining probabilistic cytoarchitectonic maps and functional imaging data. Neuroimage. 2005;25(4):1325-1335. doi:10.1016/j.neuroimage.2004.12.034.

57. Diedrichsen J, Balsters JH, Flavell J, Cussans E, Ramnani N. A probabilistic MR atlas of the human cerebellum. Neuroimage. 2009;46(1):39-46. doi:10.1016/j.neuroimage.2009.01.045.

58. Gironell A, Figueiras FP, Pagonabarraga J, et al. Gaba and serotonin molecular neuroimaging in essential tremor: a clinical correlation study. Parkinsonism Relat Disord. 2012;18(7):876-880. doi:10.1016/j.parkreldis.2012.04.024 (doi).

59. Symanski C, Shill HA, Dugger B, et al. Essential tremor is not associated with cerebellar Purkinje cell loss. Mov Disord. 2014;0(0):1-5. doi:10.1002/mds.25845.

60. Erickson-Davis CR, Faust PL, Vonsattel JP, Gupta S, Honig LS, Louis ED. "Hairy baskets" associated with degenerative Purkinje cell changes in essential tremor. J Neuropathol Exp Neurol. 2010;69(3):262-271. doi:10.1097/NEN.0b013e3181d1ad04 (doi).

61. Uusisaari M, Knöpfel T. GABAergic synaptic communication in the GABAergic and non-GABAergic cells in the deep cerebellar nuclei. Neuroscience. 2008;156(3):537-549. doi:10.1016/j.neuroscience.2008.07.060.

62. Boecker H, Weindl A, Brooks DJ, et al. GABAergic dysfunction in essential tremor: an 11C-flumazenil PET study. J Nucl Med. 2010;51(7):1030-1035. doi:10.2967/jnumed.109.074120.

63. Jahnsen H. Electrophysiological characteristics of neurones in the guinea-pig deep cerebellar nuclei in vitro. J Physiol. 1986;372:129-147. doi:10.1113/jphysiol.1986.sp016001.

64. Pinault D, Deschênes M. The origin of rhythmic fast subthreshold depolarizations in thalamic relay cells of rats under urethane anaesthesia. Brain Res. 1992;595(2):295-300. doi:10.1016/0006-8993(92)91063-K.

65. Raethjen J, Govindan RB, Kopper F, Muthuraman M, Deuschl G. Cortical involvement in the generation of essential tremor. J Neurophysiol. 2007;97(5):3219-3228. doi:10.1152/jn.00477.2006.

66. Chuang WL, Huang YZ, Lu CS, Chen RS. Reduced cortical plasticity and GABAergic modulation in essential tremor. Mov Disord. 2014;29(4):501-507. doi:10.1002/mds.25809.

67. Herrup K, Kuemerle B. The compartmentalization of the cerebellum. Annu Rev Neurosci. 1997; 20(Glickstein 1994):61-90. doi:10.1146/annurev.neuro.20.1.61.

68. Eisenman LM. Antero-posterior boundaries and compartments in the cerebellum: evidence from selected neurological mutants. Prog Brain Res. 2000;124:23-30. doi:10.1016/S0079-6123(00)24005-3.

69. Witt ST, Laird AR, Meyerand ME. Functional neuroimaging correlates of finger-tapping task variations: An ALE meta-analysis. Neuroimage. 2008;42(1):343-356. doi:10.1016/j.neuroimage.2008.04.025.

70. Diedrichsen J, Maderwald S, Küper M, et al. Imaging the deep cerebellar nuclei: A probabilistic atlas and normalization procedure. Neuroimage. 2011;54(3):1786-1794. doi:10.1016/j.neuroimage.2010.10.035.

SUPPLEMENTARY MATERIALS

FMRI AND EMG ACQUISITION

Images were acquired on a Philips 3-T MR scanner (UMCG: Intera, AMC: Ingenia, Philips, Best, The Netherlands) with SENSE-32 channel (UMCG) and SENSE-16 channel (AMC) head coils. T2*-weighted, 3D functional images were obtained using multislice echo planar imaging (EPI) with an echo time (TE) of 30 ms and a repetition time (TR) of 2000 ms. Per TR 39 axial slices, with a field of view (FOV) of 224 mm, flip angle of 5º with a 64 X 64 matrix and isotropic voxel size of 3.5 x 3.5 x 3.5 mm were acquired. To provide anatomical information, additional T1-weighted 3D anatomical scans with an axial orientation and a matrix size of 256 x 256 mm were obtained (isotropic voxel size 1 x 1 x 1 mm). EMG was recorded simultaneously (BrainProducts GmbH, Munich, Germany (UMCG) and MicroMed, Italy (AMC)) from five right arm muscles: extensor carpi ulnaris, flexor carpi radialis, extensor carpi radialis longus, flexor capri ulnaris and first dorsal interosseus. Pairs of sintered silver/silver-chloride MR-compatible EMG electrodes were placed bilaterally above the mentioned muscles. A ground electrode was placed on the left wrist joint. Further EMG recording procedures and MR correction algorithms were consistent with the methodology developed in previous studies of our group.[1-4] EMG data were corrected for MR artefacts using the MR-artefact correction algorithms (Imaging Artefact Reduction method;[5] UMCG data) embedded in the BrainVision Analyzer software (BrainProducts GmbH, Munich, Germany) and FARM (fMRI artefact reduction for motion;[2] AMC data).

FMRI AND EMG PREPROCESSING

Data was further analyzed in Matlab using custom-made scripts (Matlab R2007a, Mathworks, Natrick, USA). For each segment of 2s, the time- frequency spectrum was calculated using fast Fourier transform (FFT). The individual tremor frequency was determined for each patient and healthy control by visual inspection of the segments. Patients who had no clear spectral peak associated with tremor during the task segments were excluded from further analysis (n=16). Total spectral power in a 5Hz symmetrical band around the individual tremor peak frequency was exported for each segment and each right arm muscle, resulting in five vectors of the length of the number of scans/segments. Vectors of the three muscles with the highest power around the tremor frequency were averaged. This procedure resulted in an EMG power vector with one entry for every scan. Next, this vector was orthogonalized with respect to the motor task using Gram-Schmidt orthogonalization, to subtract the information that is already present in the block vector of the task.[6] The orthogonalized EMG vector (referred to as residual EMG or r-EMG vector) now provides a measure of additional EMG relative to the mean EMG value across the task. It represents the variation in tremor severity over time. Subsequently, the r-EMG vector was element-wise multiplied with the task block vector to obtain a vector that only has non-zeroes for the r-EMG during task, and zeroes otherwise. Finally, this vector

was scaled to the maximum value per subject to ensure that the variance was similar between subjects, convolved with the canonical HRF and used as a regressor in the fMRI design matrix.

fMRI data was analyzed using SPM12 (Wellcome Trust Centre for Neuroimaging, UCL, London, UK; http://www.fil.ion.ucl.ac.uk/spm, DCM version 12). Preprocessing consisted of realignment to correct for individual subject movement and coregistration to align all functional data to each subject's anatomical volume. A group-specific anatomic template was created (for patients and healthy controls together), using Diffeomorphic Anatomical Registration Through Exponentiated Lie algebra DARTEL for a more precise inter-subject alignment to take age-related changes in anatomy into account.[7] The functional data was normalized and smoothed using the DARTEL template and an 8-mm full-width half maximum (FWHM) Gaussian kernel. To reduce movement artefacts, the six movement parameters derived from realignment corrections were entered as covariates in each analysis. Inspection of the EMG was used to correct the block design regressor for actual on- and offsets of the motor task. As motion-related and other non-neuronal signal changes are effectively reduced by global signal regression, tissue-based signals were also used as nuisance regressors and were calculated as the average signal across all voxels within the whole-brain mask, including its first derivative.[8] Each single-subject first-level model thus consisted of two block regressor for the motor task, a residual-EMG regressor, six movement regressor and two global signal regressors.

LIST OF MODELS AND MODULATORY INPUTS

Model no.	Cerebellar outflow	SMA	PMC	Thalamus	CB V	CB VIII	M1	Model no.	Cerebellar outflow	SMA	PMC	Thalamus	CB V	CB VIII	M1	Model no.	Cerebellar outflow	SMA	PMC	Thalamus	CB V	CB VIII	M1
1	0	0	0	0	0	0	0	**45**	0	1	0	1	1	0	0	**89**	1	0	1	1	0	0	0
2	0	0	0	0	0	0	1	**46**	0	1	0	1	1	0	1	**90**	1	0	1	1	0	0	1
3	0	0	0	0	0	1	0	**47**	0	1	0	1	1	1	0	**91**	1	0	1	1	0	1	0
4	0	0	0	0	0	1	1	**48**	0	1	0	1	1	1	1	**92**	1	0	1	1	0	1	1
5	0	0	0	0	1	0	0	**49**	0	1	1	0	0	0	0	**93**	1	0	1	1	1	0	0
6	0	0	0	0	1	0	1	**50**	0	1	1	0	0	0	1	**94**	1	0	1	1	1	0	1
7	0	0	0	0	1	1	0	**51**	0	1	1	0	0	1	0	**95**	1	0	1	1	1	1	0
8	0	0	0	0	1	1	1	**52**	0	1	1	0	0	1	1	**96**	1	0	1	1	1	1	1
9	0	0	0	1	0	0	0	**53**	0	1	1	0	1	0	0	**97**	1	1	0	0	0	0	0
10	0	0	0	1	0	0	1	**54**	0	1	1	0	1	0	1	**98**	1	1	0	0	0	0	1
11	0	0	0	1	0	1	0	**55**	0	1	1	0	1	1	0	**99**	1	1	0	0	0	1	0
12	0	0	0	1	0	1	1	**56**	0	1	1	0	1	1	1	**100**	1	1	0	0	0	1	1
13	0	0	0	1	1	0	0	**57**	0	1	1	1	0	0	0	**101**	1	1	0	0	1	0	0
14	0	0	0	1	1	0	1	**58**	0	1	1	1	0	0	1	**102**	1	1	0	0	1	0	1
15	0	0	0	1	1	1	0	**59**	0	1	1	1	0	1	0	**103**	1	1	0	0	1	1	0
16	0	0	0	1	1	1	1	**60**	0	1	1	1	0	1	1	**104**	1	1	0	0	1	1	1
17	0	0	1	0	0	0	0	**61**	0	1	1	1	1	0	0	**105**	1	1	0	1	0	0	0
18	0	0	1	0	0	0	1	**62**	0	1	1	1	1	0	1	**106**	1	1	0	1	0	0	1
19	0	0	1	0	0	1	0	**63**	0	1	1	1	1	1	0	**107**	1	1	0	1	0	1	0
20	0	0	1	0	0	1	1	**64**	0	1	1	1	1	1	1	**108**	1	1	0	1	0	1	1
21	0	0	1	0	1	0	0	**65**	1	0	0	0	0	0	0	**109**	1	1	0	1	1	0	0
22	0	0	1	0	1	0	1	**66**	1	0	0	0	0	0	1	**110**	1	1	0	1	1	0	1
23	0	0	1	0	1	1	0	**67**	1	0	0	0	0	1	0	**111**	1	1	0	1	1	1	0
24	0	0	1	0	1	1	1	**68**	1	0	0	0	0	1	1	**112**	1	1	0	1	1	1	1
25	0	0	1	1	0	0	0	**69**	1	0	0	0	1	0	0	**113**	1	1	1	0	0	0	0
26	0	0	1	1	0	0	1	**70**	1	0	0	0	1	0	1	**114**	1	1	1	0	0	0	1
27	0	0	1	1	0	1	0	**71**	1	0	0	0	1	1	0	**115**	1	1	1	0	0	1	0
28	0	0	1	1	0	1	1	**72**	1	0	0	0	1	1	1	**116**	1	1	1	0	0	1	1
29	0	0	1	1	1	0	0	**73**	1	0	0	1	0	0	0	**117**	1	1	1	0	1	0	0
30	0	0	1	1	1	0	1	**74**	1	0	0	1	0	0	1	**118**	1	1	1	0	1	0	1
31	0	0	1	1	1	1	0	**75**	1	0	0	1	0	1	0	**119**	1	1	1	0	1	1	0
32	0	0	1	1	1	1	1	**76**	1	0	0	1	0	1	1	**120**	1	1	1	0	1	1	1
33	0	1	0	0	0	0	0	**77**	1	0	0	1	1	0	0	**121**	1	1	1	1	0	0	0
34	0	1	0	0	0	0	1	**78**	1	0	0	1	1	0	1	**122**	1	1	1	1	0	0	1

LIST OF MODELS AND MODULATORY INPUTS *(Continued)*

Model no.	Cerebellar outflow	SMA	PMC	Thalamus	CB V	CB VIII	M1	Model no.	Cerebellar outflow	SMA	PMC	Thalamus	CB V	CB VIII	M1	Model no.	Cerebellar outflow	SMA	PMC	Thalamus	CB V	CB VIII	M1
35	0	1	0	0	0	1	0	**79**	1	0	0	1	1	1	0	**123**	1	1	1	1	0	1	0
36	0	1	0	0	0	1	1	**80**	1	0	0	1	1	1	1	**124**	1	1	1	1	0	1	1
37	0	1	0	0	1	0	0	**81**	1	0	1	0	0	0	0	**125**	1	1	1	1	1	0	0
38	0	1	0	0	1	0	1	**82**	1	0	1	0	0	0	1	**126**	1	1	1	1	1	0	1
39	0	1	0	0	1	1	0	**83**	1	0	1	0	0	1	0	**127**	1	1	1	1	1	1	0
40	0	1	0	0	1	1	1	**84**	1	0	1	0	0	1	1	**128**	1	1	1	1	1	1	1
41	0	1	0	1	0	0	0	**85**	1	0	1	0	1	0	0								
42	0	1	0	1	0	0	1	**86**	1	0	1	0	1	0	1								
43	0	1	0	1	0	1	0	**87**	1	0	1	0	1	1	0								
44	0	1	0	1	0	1	1	**88**	1	0	1	0	1	1	1								

FULL DETAILS DCM COUPLING PARAMETERS BASED ON BAYESIAN MODEL AVERAGING

The posterior densities of the parameters are calculated across subjects and across the winning halve of models. More weight is given to the models with the highest posterior probability according to Bayes' rule.[9] The resulting coupling parameters represent connection strengths.[10] The posterior distributions are calculated using a Gibbs sampling approach by drawing samples from a multinomial distribution of posterior beliefs for the included models.[9] Subsequently, posterior means and standard deviations of parameters were obtained and tested for significance using two-tailed *t*-test. Significance levels are corrected for multiple comparisons using false discovery rate (FDR) correction.[11] Positive coupling parameters suggest a facilitation of neural activity, whereas negative coupling parameters can be interpreted as inhibition of neural activity. The coupling parameter unit is Hertz (Hz), reflecting the amount of activity that flows from one region into another per second.

DCM A-MATRIX – ENDOGENOUS CONNECTIVITY BASED ON BAYESIAN MODEL AVERAGING

Parameter estimate:	Mean	SD	*t*-value	p value
M1 → M1	-0,4450	0,0367	51,445203	**0,00000**
M1 → SMA	-0,1275	0,0513	10,544575	**0,00000**
M1 → PMC	-0,0348	0,0424	3,4821674	0,00309
M1 → Thal	-0,1471	0,0388	16,084857	**0,00000**
M1 → CBV	-0,1324	0,0344	16,329233	**0,00000**
M1 → CBVIII	-0,1252	0,0346	15,351983	**0,00000**
SMA → SMA	-0,4295	0,0339	53,751897	**0,00000**
SMA → M1	0,2867	0,0299	40,681107	**0,00000**
SMA → PMC	0,1370	0,0407	14,281125	**0,00000**
SMA → Thal	0,2454	0,0348	29,917932	**0,00000**
SMA → CBV	0,2550	0,0352	30,735039	**0,00000**
SMA → CBVIII	0,1929	0,0280	29,228764	**0,00000**
PMC → PMC	-0,4650	0,0369	53,467951	**0,00000**
PMC → M1	0,0905	0,0419	9,1636989	**0,00000**
PMC → SMA	0,0838	0,0502	7,0823364	**0,00000**
PMC → Thal	0,0808	0,0495	6,925361	**0,00000**
PMC → CBV	0,1075	0,0456	10,001839	**0,00000**
PMC → CBVIII	0,1461	0,0417	14,864504	**0,00000**
Thal → Thal	-0,6150	0,0346	75,41003	**0,00000**
Thal → M1	0,1330	0,0468	12,057077	**0,00000**
Thal → SMA	0,4972	0,0843	25,023024	**0,00000**
Thal → PMC	0,3105	0,0684	19,259356	**0,00000**
CBV → CBV	-0,4155	0,0352	50,081311	**0,00000**
CBV → Thal	-0,0598	0,0410	6,1880467	**0,00001**
CBV → CBVIII	0,0357	0,0508	2,9815408	0,00892
CBVIII → CBVIII	-0,4301	0,0392	46,54489	**0,00000**
CBVIII → Thal	-0,0484	0,0541	3,7956342	0,00157
CBVIII → CBV	0,0721	0,0501	6,1056765	**0,00001**

Mean endogenous connectivity parameters, statistical significance determined by one sample two-tailed *t*-test. Full endogenous connectivity was assumed with the exemption of connections between cerebellar regions and the thalamus (only unidirectional from cerebellum to thalamus) and between cortical and cerebellar regions (only unidirectional from cortical to cerebellar regions) based on neuronal tracing studies in macaque monkeys,[12] leaving 28 connections. FDR-corrected significant parameters in bold. M1: primary motor cortex; SMA: supplementary motor area; PMC: premotor cortex; Thal: thalamus; CBV: cerebellar lobule V; CBVIII: cerebellar lobule VIII.

DCM C-MATRIX – DIRECT (TASK) INPUT

Parameter estimate:	Mean	SD	*t*-value	p value
Task input SMA (with silent reading task)	0,1021	0,0100	43,317361	0,00000
Task input SMA (without silent reading task)	0,0684	0,0087	33,355934	0,00000
Task input PMC (with silent reading task)	0,0446	0,0102	18,551154	0,00000
Task input PMC (without silent reading task)	0,0450	0,0085	22,461039	0,00000

Mean influence of task input, statistical significance determined by one sample two-tailed *t*-test. FDR-corrected significant parameters in bold. SMA: supplementary motor area; PMC: premotor cortex.

ONE SAMPLE T-TEST – MOTOR TASK CONJUNCTION ANALYSIS OF ESSENTIAL TREMOR PATIENTS AND HEALTHY CONTROLS

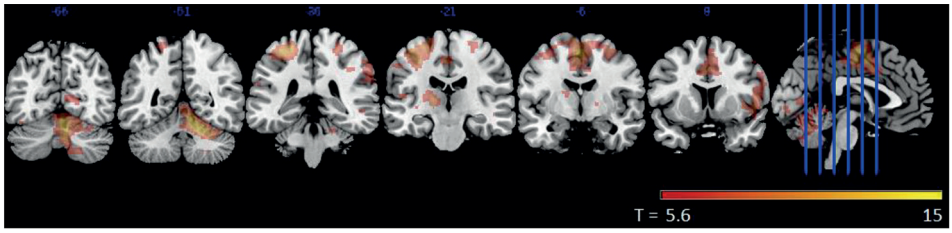

Region	Hemisphere	*t*-value	$P_{FWE\text{-}corr}$	Cluster size	x,y,z in mm		
Cerebellar lobule IV	Right	14.94	<0.001	3841	4	54	-21
Cerebellar lobule V	Right	14.16	<0.001		14	-50	-19
Cerebellar lobule VI	Right	13.92	<0.001		22	-50	-25
Primary motor cortex	Left	14.52	<0.001	5048	-28	-28	53
Supplementary motor area	Left	14.04	<0.001		-2	-8	57
Primary motor cortex	Left	13.49	<0.001		-36	-32	61

Task-related activity – results of a one sample *t*-test – conjunction analysis of essential tremor patients and healthy controls. The six most significant peak-voxels are listed. Cerebellar lobule VIII is located within the most significant cluster with peak-region cerebellar lobule IV.

ONE SAMPLE T-TEST – FUNCTIONAL CONNECTIVITY MAPS PER SEED REGION, CONJUNCTION ANALYSIS OF ESSENTIAL TREMOR PATIENTS AND HEALTHY CONTROLS

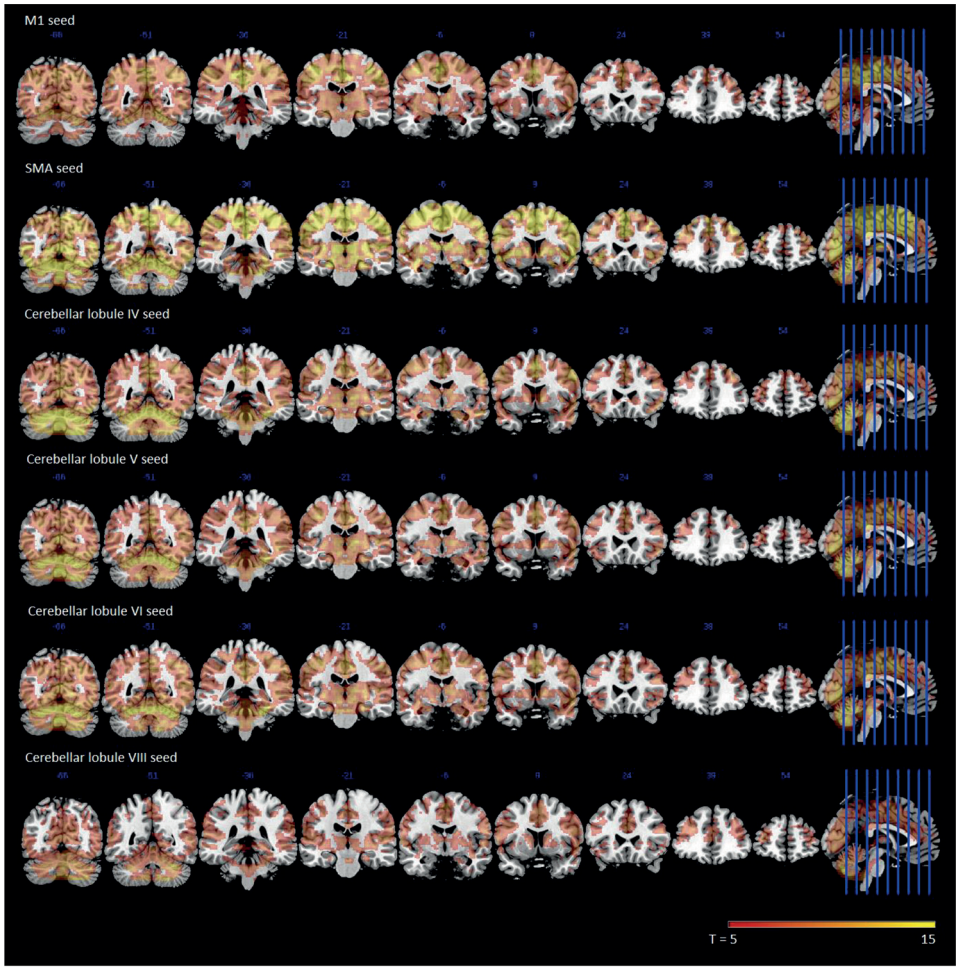

SUPPLEMENTARY REFERENCES

1. Van Duinen H, Zijdewind I, Hoogduin H, Maurits N. Surface EMG measurements during fMRI at 3T: Accurate EMG recordings after artifact correction. Neuroimage. 2005;27(1):240-246. doi:10.1016/j.neuroimage.2005.04.003.
2. van der Meer JN, Tijssen M a J, Bour LJ, van Rootselaar a F, Nederveen a J. Robust EMG-fMRI artifact reduction for motion (FARM). Clin Neurophysiol. 2010;121(5):766-776. doi:10.1016/j.clinph.2009.12.035.
3. Contarino MF, Groot PFC, van der Meer JN, et al. Is there a role for combined EMG-fMRI in exploring the pathophysiology of essential tremor and improving functional neurosurgery? Draganski B, ed. PLoS One. 2012;7(10):e46234. doi:10.1371/journal.pone.0046234.
4. Van Rootselaar AF, Maurits NM, Renken R, et al. Simultaneous EMG-functional MRI recordings can directly relate hyperkinetic movements to brain activity. Hum Brain Mapp. 2008;29(12):1430-1441. doi:10.1002/hbm.20477.
5. Allen PJ, Josephs O, Turner R. A method for removing imaging artifact from continuous EEG recorded during functional MRI. Neuroimage. 2000;12(2):230-239. doi:10.1006/nimg.2000.0599.
6. Van Rootselaar AF, Renken R, De Jong BM, Hoogduin JM, Tijssen M a J, Maurits NM. fMRI analysis for motor paradigms using EMG-based designs: A validation study. Hum Brain Mapp. 2007;28(11):1117-1127. doi:10.1002/hbm.20336.
7. Ashburner J. A fast diffeomorphic image registration algorithm. Neuroimage. 2007;38(1):95-113. doi:10.1016/j.neuroimage.2007.07.007.
8. Power JD, Mitra A, Laumann TO, Snyder AZ, Schlaggar BL, Petersen SE. Methods to detect, characterize, and remove motion artifact in resting state fMRI. Neuroimage. 2014;84:320-341. doi:10.1016/j.neuroimage.2013.08.048.
9. Penny WD, Stephan KE, Daunizeau J, et al. Comparing families of dynamic causal models. PLoS Comput Biol. 2010;6(3). doi:10.1371/journal.pcbi.1000709.
10. Friston KJ, Harrison L, Penny W. Dynamic causal modelling. Neuroimage. 2003;19(4):1273-1302. doi:10.1016/S1053-8119(03)00202-7.
11. Ćurcić-Blake B, Swart M, Aleman A. Bidirectional information flow in frontoamygdalar circuits in humans: A dynamic causal modeling study of emotional associative learning. Cereb Cortex. 2012;22(2):436-445. doi:10.1093/cercor/bhr124.
12. Middleton FA, Strick PL. Basal ganglia and cerebellar loops: Motor and cognitive circuits. In: Brain Research Reviews. Vol 31. ; 2000:236-250. doi:10.1016/S0165-0173(99)00040-5.